J|A|C|S ARTICLES

Published on Web 03/24/2010

Protein Aggregation in Crowded Environments

Duncan A. White,[†,‡] Alexander K. Buell,[‡] Tuomas P. J. Knowles,[‡] Mark E. Welland,[‡] and Christopher M. Dobson*[,†]

Department of Chemistry, University of Cambridge, Cambridge, U.K. CB2 1EW, and Nanoscience Centre, University of Cambridge, Cambridge, U.K. CB3 0FF

Received December 1, 2009; E-mail: cmd44@cam.ac.uk

Abstract: The physicochemical parameters of biomolecules are the key determinants of the multitude of processes that govern the normal and aberrant behavior of living systems. A particularly important aspect of such behavior is the role it plays in the self-association of proteins to form organized aggregates such as the amyloid or amyloid-like fibrils that are associated with pathological conditions including Alzheimer's disease and Type II diabetes. In this study we describe quantitative quartz crystal microbalance measurements of the kinetics of the growth of amyloid fibrils in a range of crowded environments and in conjunction with theoretical predictions demonstrate the existence of general relationships that link the propensities of protein molecules to aggregate with fundamental parameters that describe their specific structures and local environments.

Introduction

Amyloid fibrils are highly ordered protein aggregates that are associated both with biological self-assembly and with the formation of functional structures.[1] They are best known in connection with a range of neurodegenerative disorders and prion diseases as well as with other forms of abnormal behavior including the deposition within organs such as the liver, spleen, and heart of large quantities of proteins in various forms of systemic amyloidoses.[2,3] It has been shown in a wide range of studies that the conversion of normally soluble proteins into amyloid structures can be promoted by nonphysiological solution conditions such as extremes of temperature or pH or the addition of nanoparticles.[2,4,5]

In a living cell, however, additional physicochemical parameters modulate protein self-assembly, one of the most intriguing of which is the effect of macromolecular crowding as the cellular environment contains many volume-excluding macromolecules such as proteins, polysaccharides, and lipids. In addition to specific interactions within this environment, nonspecific effects can perturb the dynamics of all biochemical processes on which living systems depend.[6,7] Considerable progress has been made in understanding the effects of macromolecular crowding on protein folding, conformation, and function.[8−10] The aggregation of proteins, however, is a somewhat more complex process in that the aggregation propensity of a system is dependent on a combination of distinct effects such as sequence, monomer conformation, nucleation rate, effective protein concentration, intermolecular interactions, diffusive properties, and the action of species such as chaperone molecules.[11−19] The magnitude of such effects is dependent on the physical and chemical properties of the proteins involved and the macromolecules that give rise to crowding. Despite this apparent complexity, we show here that by combining a biosensor assay with a theoretical analysis, both of which consider exclusively fibril elongation, it is possible to identify generic trends that describe well the response of amyloid growth to crowding as a function of only a few key parameters characteristic of the protein structure and the crowded milieu.

Experimental measurements in crowded systems are inherently challenging as the presence of a large excess of spectator molecules has the potential to influence or conceal any signal from a specific component that is used to monitor a given reaction. Crowded environments are also known to modify profoundly the association of components, for example through attractive entropic interactions such as the depletion pressure that results from the entropically favorable overlap of the regions

[†] Department of Chemistry.
[‡] Nanoscience Centre.

(1) Fowler, D. M.; Koulov, A. V.; Alory-Jost, C.; Marks, M. S.; Balch, W. E.; Kelly, J. W. *PLoS Biol.* **2006**, *4*, e6.
(2) Dobson, C. M. *Nature* **2003**, *426*, 884–890.
(3) Aguzzi, A.; Haass, C. *Science* **2003**, *302*, 814–818.
(4) Perálvarez-Marín, A.; Barth, A.; Gräslund, A. *J. Mol. Biol.* **2008**, *379*, 589–596.
(5) Cabaleiro-Lago, C.; Quinlan-Pluck, F.; Lynch, I.; Lindman, S.; Minogue, A. M.; Thulin, E.; Walsh, D. M.; Dawson, K. A.; Linse, S. *J. Am. Chem. Soc.* **2008**, *130*, 15437–15443.
(6) Zimmerman, S. B.; Trach, S. O. *J. Mol. Biol.* **1991**, *222*, 599–620.
(7) Hall, D.; Dobson, C. M. *FEBS Lett.* **2006**, *580*, 2584–2590.
(8) van den Berg, B.; Wain, R.; Dobson, C. M.; Ellis, R. J. *EMBO J.* **2000**, *19*, 3870–3875.
(9) Cheung, M. S.; Klimov, D.; Thirumalai, D. *Proc. Natl. Acad. Sci. U.S.A.* **2005**, *102*, 4753–4758.
(10) Homouz, D.; Perham, M.; Samiotakis, A.; Cheung, M. S.; Wittung-Stafshede, P. *Proc. Natl. Acad. Sci. U.S.A.* **2008**, *105*, 11754–11759.
(11) Pedersen, J. S.; Otzen, D. E. *Protein Sci.* **2008**, *17*, 2–10.
(12) Kuriyan, J.; Eisenberg, D. *Nature* **2007**, *450*, 983–990.
(13) Cellmer, T.; Henry, E. R.; Hofrichter, J.; Eaton, W. A. *Proc. Natl. Acad. Sci. U.S.A.* **2008**, *105*, 18320–18325.
(14) Hwang, W.; Zhang, S.; Kamm, R. D.; Karplus, M. *Proc. Natl. Acad. Sci. U.S.A.* **2004**, *101*, 12916–12921.
(15) Krishnan, R.; Lindquist, S. L. *Nature* **2005**, *435*, 765–772.
(16) Asakura, S.; Oosawa, F. *J. Polym. Sci.* **1958**, *33*, 183–192.
(17) Ellis, R. J.; Minton, A. P. *Biol. Chem.* **2006**, *387*, 485–497.
(18) Hartl, F. U. *Nature* **1996**, *381*, 571–579.
(19) Hammarström, P.; Jiang, X.; Hurshman, A. R.; Powers, E. T.; Kelly, J. W. *Proc. Natl. Acad. Sci. U.S.A.* **2002**, *99*, 16427–16432; Suppl. 4.

10.1021/ja909997e

surrounding two particles into which cosolutes are unable to penetrate.[16] A consequence of such effects is that the stoichiometry and binding affinity of large reporter molecules to amyloid structures are susceptible to significant variability, a problem that is complicated further by recent evidence concerning the limitations of traditional dye-based assays.[20] To achieve quantitative measurements in a crowded environment, therefore, we have focused in the present study on a label-free measurement approach based on a quartz crystal microbalance (QCM) assay that has recently been developed as a general method of monitoring with high accuracy the elongation of amyloid fibrils consequent upon the addition of their monomeric precursor.[21−23]

Results and Discussion

QCM Assay. The QCM assay specifically monitors the elongation of an ensemble of seed fibrils that are attached to a quartz crystal sensor surface by measuring the increase in mass associated with the attachment of individual molecules; the latter results in a negative shift in the resonant frequency of the quartz crystal sensor[24] that can be measured to a high level of accuracy. Crucially, the fact that multiple measurements can be made on the same ensemble of seed fibrils and that stochastic processes such as nucleation and breakage do not contribute to these measurements substantially increases the accuracy and reproducibility of this approach relative to traditional solution methods that monitor the quantity of fibrillar species present under given conditions.[25] Repeated atomic force microscopy imaging of the sensor surface showed that the lengths of covalently bound fibrils do not decrease over time scales an order of magnitude greater than the experiment time. Additionally nucleation events also play no significant role in our measurements as fibril growth is observed as a linear decrease in resonant frequency upon exposure to monomeric protein (Figure 1).

Biosensing Protein Fibril Elongation in Crowded Environments. A primary advantage of the QCM assay is that measurements of fibril growth may be performed repeatedly on the same ensemble of fibrils (Figure 1C, G, K, and O); the deviation of the repeat measurements is typically within 10% of the mean elongation rate. We describe here the operation of QCM assays in crowded environments (Figure 1D, H, L, and P).[21] Initially, protein seed fibrils on the sensor surface are exposed to a buffer solution, and the resonant frequency does not change as a function of time (I). Following exposure to a solution containing a macromolecular cosolute (II), the sensor rapidly adapts to the increased viscosity[26] and a new stable baseline frequency is obtained. We can at this point verify that there is no binding of the cosolute to the fibrils or the sensor surface by reverting to the pure buffer solution (I′), following which the resonant frequency is observed to return to its initial value. A second exposure to a solution containing inert macromolecules (II′) then reproduces the initial viscosity-driven shift in resonant frequency, illustrating the reliability of the biosensor approach. The system is now ready for amyloid growth measurements that are achieved by exposing the surface to a solution containing both soluble protein and inert macromolecules; the addition of protein monomers to the ends of the surface-bound fibrils can then be followed in real time through the associated increase in surface-bound hydrodynamic mass (III). Finally, when the protein solution is replaced with pure buffer, the growth ceases in the absence of available protein monomers, and the number of molecules that have attached themselves to the fibrils can be evaluated as a function of time by calculating the mass change from the difference in the resonant frequencies before and after growth (I′ and I″, respectively). A comparison can then be made with data from analogous measurements of the rate of fibril elongation in the absence of crowding agents. We find in the present study that the linear slopes corresponding to the growth phases within the crowded environment (III) yield growth rates similar to those obtained from evaluation of the differences in the pre- and postgrowth baselines (I′ and I″), illustrated by the dashed lines; strongly supporting the validity of the measurements.

Volume Excluding Cosolutes. Having established the accuracy and robustness of QCM assays under crowded conditions, we carried out systematic studies of the elongation rates of a range of proteins as a function of cosolute concentration in the presence of high molecular weight forms of polysaccharide and poly(ethylene glycol) (PEG) molecules. Figure 2A shows, as an example, data for bovine insulin fibrils where the addition of high molecular weight cosolutes such as dextran (200 kDa) and PEG (200 kDa) can be seen to accelerate the rate of fibril elongation despite a concurrent increase in solvent relative viscosity from 1 to 4.3 mPas in the case of dextran as the concentration was increased from 0 to 50 mg/mL. To interpret the significance of these results, we adopted scaled particle theory[27] to calculate the changes in the thermodynamic activities of proteins as a result of the crowded conditions in terms of the changes in available volume (see Experimental Section).[28] For example, an insulin molecule placed into a solution of 50 mg/mL dextran will have an activity coefficient of 1.4, and a protein fibril with length 50 nm and radius 2.25 nm has an activity coefficient of 2775.0 under the same conditions, according to eq 4. If we combine these particles into a single elongated fibril, the activity coefficient rises to 3908.2 and we can relate these values according to eqs 2 and 7 to give a relative elongation rate of 1.3.

It is particulary important to note here that scaled particle theory in the current form predicts only the effects of crowding on fibril elongation, and to date this model has received only limited success in the literature in describing accurately data from solution measurements,[29] most likely due to stochastic contributions from secondary nucleation events such as fibril breakage.[30] The QCM assay does not suffer from such stochastic processes and has the ability to measure directly the elongation

(20) Khurana, R.; Uversky, V. N.; Nielsen, L.; Fink, A. L. *J. Biol. Chem.* **2001**, *276*, 22715–22721.
(21) Knowles, T. P. J.; Shu, W.; Devlin, G. L.; Meehan, S.; Auer, S.; Dobson, C. M.; Welland, M. E. *Proc. Natl. Acad. Sci. U.S.A.* **2007**, *104*, 10016–10021.
(22) Buell, A. K.; Tartaglia, G. G.; Birkett, N. R.; Waudby, C. A.; Vendruscolo, M.; Salvatella, X.; Welland, M. E.; Dobson, C. M.; Knowles, T. P. J. *ChemBioChem* **2009**, *10*, 1309–1312.
(23) White, D. A.; Buell, A. K.; Dobson, C. M.; Welland, M. E.; Knowles, T. P. J. *FEBS Lett.* **2009**, *583*, 2587–2592.
(24) Sauerbrey, G. *Z. Phys.* **1959**, *155*, 206–222.
(25) Naiki, H.; Higuchi, K.; Hosokawa, M.; Takeda, T. *Anal. Biochem.* **1989**, *177*, 244–249.
(26) Kanazawa, K. K.; Gordon, J. G. *Anal. Chem.* **1985**, *57*, 1770–1771.
(27) Ogston, A. G. *Trans. Faraday Soc.* **1958**, *54*, 1754–1757.
(28) Minton, A. P. *Mol. Cell. Biochem.* **1983**, *55*, 119–140.
(29) Hatters, D. M.; Minton, A. P.; Howlett, G. J. *J. Biol. Chem.* **2002**, *277*, 7824–7830.
(30) Knowles, T. P. J.; Waudby, C. A.; Devlin, G. L.; Cohen, S. I. A.; Aguzzi, A.; Vendruscolo, M.; Terentjev, E. M.; Welland, M. E.; Dobson, C. M. *Science* **2009**, *326*, 1533–1537.
(31) Oliva, A.; Fariña, J.; Llabrés, M. *J. Chromatogr., B: Biomed. Sci. Appl.* **2000**, *749*, 25–34.
(32) Laurent, T. C.; Killander, J. *J. Chromatogr. A* **1964**, *14*, 303–303.
(33) Atha, D. H.; Ingham, K. C. *J. Biol. Chem.* **1981**, *256*, 12108–12117.

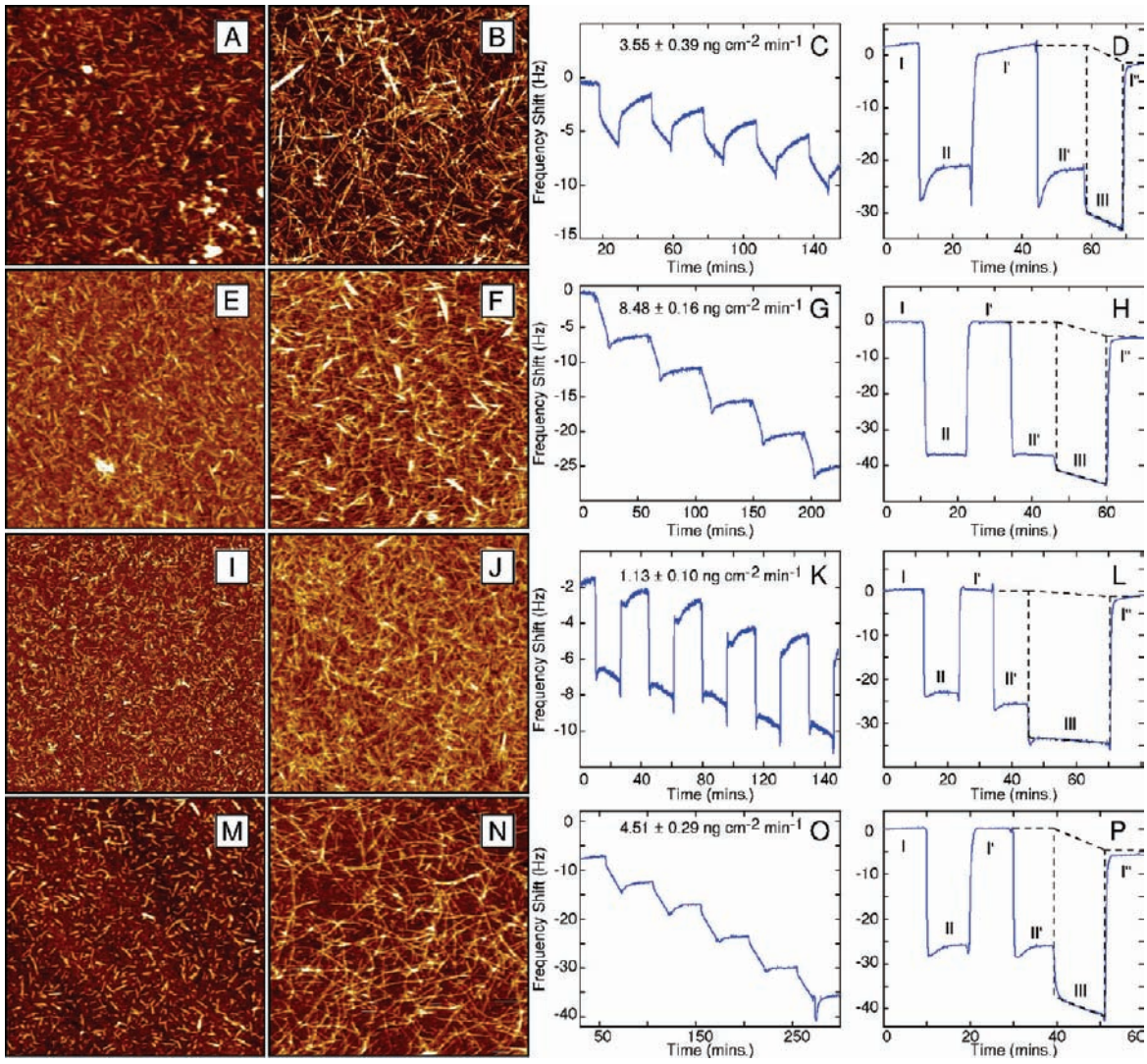

Figure 1. Amyloid fibril growth measured using the QCM technique. Several proteins were studied: (A−D) the insulin B-chain, (E−H) bovine insulin, (I−L) hen egg white lysozyme, and (M−P) human α-synuclein. The first and second columns show tapping mode atomic force microscopy images of the QCM sensor surfaces before and after exposure to monomeric protein, respectively (Image width, 4 μm). The third column demonstrates repeated exposure of soluble protein to the same ensemble of seed fibrils for each protein system, revealing the reproducibility of the QCM assay; the mean growth rates and standard deviations are shown for each system. The final column illustrates QCM measurements in crowded environments (I) pure buffer, (II) buffer and cosolute, and (III) buffer, cosolute, and monomeric protein.

of fibrils, making it ideally suited to measurements of the effects of macromolecular crowding on amyloid fibril growth.

The effect of macromolecular crowding on the rate of fibril growth is reported here as a relative rate between elongation in a crowded environment and that in an ideal solution; relative rates of >1.0 are therefore indicative of enhancement and <1.0 of inhibition. In the current model, the geometry of high molecular weight cosolutes is approximated as a random array of rigid rods, the soluble protein molecules are treated as hard spheres, and the growing amyloid fibrils as rigid spherocylinders (Figure 2E).[27] By taking the characteristic dimensions of insulin fibril formation in dextran or PEG (monomer radius 1.3 nm,[31] dextran chain radius 0.675 nm,[32] PEG chain radius 0.22 nm,[33] specific exclusion volume of dextran 0.0008 L/g,[34] specific exclusion volume of PEG 0.00084 L/g,[33] radius of an insulin fibril 2.25 nm,[35] and the increase in length of a fibril on the addition of an insulin monomer, Δ, as 0.47 nm[21,36]), eq 5 can be used to perform parameter-free predictions of the relative rate of insulin fibril elongation, under crowded conditions. The predictions are found to be in excellent agreement with the observed data for both PEG (200 kDa) and dextran (200 kDa) (Figure 2A).

Scaled particle theory may therefore be used successfully to make parameter-free predictions of the effects of crowding on amyloid fibril growth, although it should be noted that large viscosities prevent measurements under very high cosolute concentrations in the flow cell of the QCM and that discrepancies in the exact functional forms of the curves may be explained by viscosity contributions that are neglected in scaled

(34) Rivas, G.; Fernandez, J. A.; Minton, A. P. *Biochemistry* **1999**, *38*, 9379–9388.
(35) Ortiz, C.; Zhang, D.; Ribbe, A. E.; Xie, Y.; Ben-Amotz, D. *Biophys. Chem.* **2007**, *128*, 150–155.
(36) Jiménez, J. L.; Nettleton, E. J.; Bouchard, M.; Robinson, C. V.; Dobson, C. M.; Saibil, H. R. *Proc. Natl. Acad. Sci. U.S.A.* **2002**, *99*, 9196–9201.
(37) Wilkins, D. K.; Grimshaw, S. B.; Receveur, V.; Dobson, C. M.; Jones, J. A.; Smith, L. J. *Biochemistry* **1999**, *38*, 16424–16431.

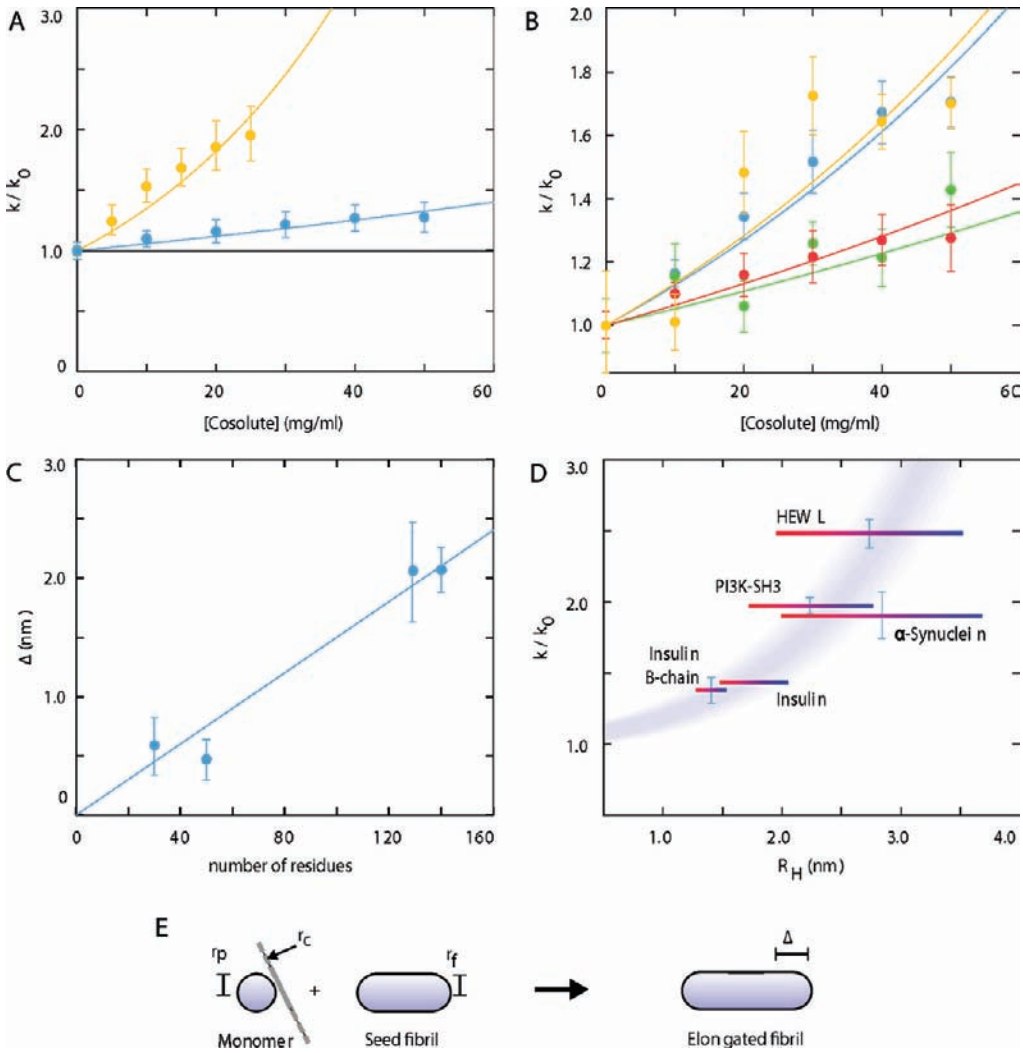

Figure 2. Amyloid fibril growth in crowded media composed of high-aspect ratio polymer chains. (A) Relative insulin fibril elongation rate in the presence of dextran (200 kDa) (blue) and PEG (200 kDa) (orange). Solid lines are parameter-free predictions using eq 5 for dextran (200 kDa) with $r_c = 0.675$ nm[34] and $\upsilon = 0.0008$ L/g and for PEG (200 kDa) with $r_c = 0.22$ nm[33] and $\upsilon = 0.00084$ L/g.[33] (B) Relative fibril elongation rates for bovine insulin (red), the insulin B-chain (green), human α-synucelin (blue), and hen egg white lysozyme (orange) in the presence of dextran (200 kDa). Solid lines are fits to eq 5 with Δ as a free parameter. (C) The increase in fibril length upon monomer addition, Δ, as a function of the number of amino acid residues fitted with a linear regression as a guide to the eye; error bars are the standard deviations from the fits in panel B. (D) Relative growth rates as a function of the protein hydrodynamic radius in the presence of 50 mg/mL dextran (200 kDa). Horizontal error bars represent the variation of protein radius from fully folded (red) to unfolded (blue),[37] and the blue band represents the prediction from scaled particle theory using eq 5 by varying r_f between 0 and 5 nm in accordance with AFM images of fibril heights. (E) Schematic representation of the particle geometries used in scaled particle theory illustrating their characteristic dimensions.

particle theory. In addition to parameter-free predictions of insulin fibril growth, we also studied several other protein systems where the increases in fibril length upon monomer addition, Δ, were unknown. We then used Δ as a free parameter to fit data from the insulin B-chain, α-synuclein, and lysozyme, (Figure 2B), and found a high degree of correlation between Δ and the number of amino acid residues in the polypeptide, which we have fitted using a simple linear regression as a guide to the eye, (Figure 2C). This approach is not as direct or accurate as structural methods such as AFM or EM to determine Δ,[21,36] but it provides substantial evidence that subtle correlations can still be observed in highly complex environments.

Crucially, scaled particle theory also predicts an increase in the relative rate of fibril elongation as the effective radius of the soluble protein precursor molecule increases. To test this prediction, we explored the effect of a high molecular weight dextran (200 kDa, at 50 mg/mL) on a series of five proteins of different molecular weights (Figure 2B). The hydrodynamic radii of the proteins were calculated from pulsed field gradient NMR studies of a range of native and denatured proteins.[37] Experimentally, we found that the rate of amyloid fibril growth was accelerated for all proteins studied here in the presence of dextran (200 kDa) and furthermore that there is a good correlation between the relative rates and the protein hydrodynamic radii as described by scaled particle theory (eq 5). Our results also show that the change in activity coefficients of protein molecules in the presence of cosolutes of a much larger size is well captured by the entropic interactions described by scaled particle theory, which are associated with the changes in volume available to the reactants and products. By contrast, changes in the viscosity of the solution do not have a pronounced influence on the rate of elongation under the conditions studied here, a finding that is consistent with the notion that the dynamics of crowding by large polymers are characterized by time scales larger than those governing the diffusional transport of the protein monomers.

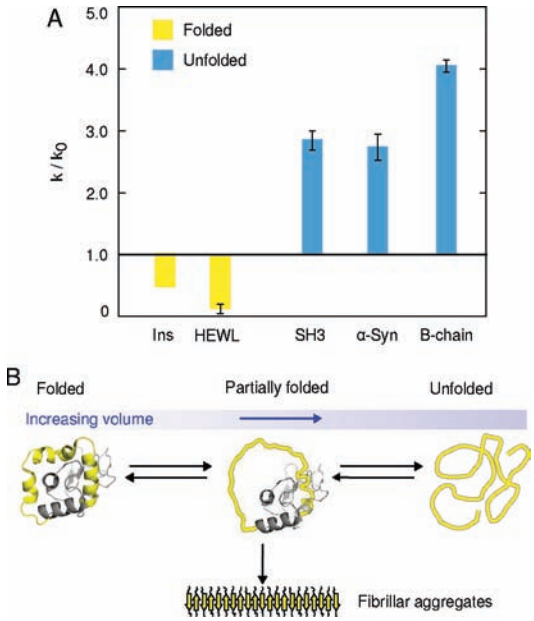

Figure 3. Amyloid growth in the presence of a stabilizing osmolyte, glucose. (A) Relative elongation rates for five amyloid systems (two natively folded, three natively unfolded) in the presence of 200 mg/mL glucose. (B) Hypothesized process for amyloid formation from a natively folded or unfolded protein, involving an initial increase or reduction in volume of the polypeptide, respectively.

Osmolytes. A further series of studies of fibril growth was carried out in the presence of glucose (180 Da), which was found to have very different effects on the rate of fibril growth of different proteins, in contrast to the universal acceleration in the presence of large molecular weight cosolutes discussed above. Remarkably, as described below, the differential effects on the fibril growth rates of the different proteins are well captured by considering, in addition to the relative sizes of the cosolutes, only a single parameter, namely, the degree of structure that the precursor proteins possess in their soluble forms. Scaled particle theory predicts that the relative rate of fibril elongation will decrease as the radius of the cosolute molecules decreases. For small cosolutes therefore, entropic interactions described by scaled particle theory become negligible, and any effects of cosolutes on the fibril growth rate must stem from other physicochemical phenomena.

Osmolytes, small organic solutes that are found in osmotically stressed environments, have been reported to stabilize the compact states of proteins by preferential exclusion of the osmolyte from the surface of the protein.[38] In particular, the presence of oligosaccharides has been shown to inhibit aggregation processes that involve an increase in the volume of a protein from the native state to the aggregation-prone transition state of the self-association reaction[39] (Figure 3C). In accord with this finding we observe here that fibril growth is inhibited by the presence of glucose only for proteins that retain a significant degree of globular structure and hence require a volume increase associated with the unfolding step prior to aggregation (e.g., in the present study both insulin and hen egg white lysozyme (HEWL) at pH 2.0 come into this category) (Figure 3B). By contrast, for proteins lacking persistent structure that are expected to have aggregation-prone transition states more compact than the native conformation (e.g., here, PI3K-SH3 and the insulin B-chain at pH 2.0 and α-synuclein[40] at pH 7.4), an increase in the relative rate of fibril elongation is observed experimentally in the presence of 200 mg/mL glucose. On the basis of these findings, it is interesting to note that previous investigations using fluorescent reporter molecules are in agreement with our observations that the aggregation of unfolded polypeptides is accelerated by low molecular weight cosolutes and osmolytes (such as trimethyl amine *N*-oxide, trehalose, and poly(ethylene glycol)),[41−44] while the aggregation of proteins that retain a degree of structure under aggregating conditions is inhibited.[21,45]

We have shown here that the complex effects of macromolecular crowding on the growth of amyloid fibrils can be well described on the basis of established physical principles using a combination of osmolytic effects and entropic interactions. We have shown experimentally that with this framework it is possible to predict accurately the susceptibility of a range of proteins with different structural properties to aggregate in various *in vitro* environments. These experiments are complemented by theoretical analysis that predicts exponential increases in the rates of self-association reactions with increasing concentrations of cosolute and with increasing protein radii. If we consider the rate of addition to an amyloid fibril of a protein of ca. 300 amino acids that we approximate as a sphere of radius 3.0 nm, eq 6 predicts that the relative rate will increase by a factor of 15 in the presence of 300 mg/mL of spherical cosolutes, also of radius 3.0 nm, values characteristic of the cellular environment.[6] This ambitious extrapolation neglects all viscosity contributions that are likely to inhibit the predicted acceleration, but it is interesting that such an acceleration in rate is greater than the acceleration of the growth rate observed as the pH is reduced from 7.0 to 1.6 during the formation of insulin fibrils.[46] The ability to modulate reaction kinetics to such large extents, therefore, supports the view that macromolecular crowding is likely to be an important consideration for biochemical reactions in living systems in general and for protein aggregation in particular.[17] The present study shows that a detailed knowledge and understanding of the magnitude of these effects is accessible using a combination of sophisticated experimental techniques and quantitative predictions based on the fundamental physicochemical characteristics of the system.

Experimental Section

Protein Expression and Purification. Wild type α-synuclein and PI3K-SH3 were produced by overexpression in *Escherichia coli* BL21 cells following methods described previously.[22,47,48] Insulin, the oxidized form of the insulin B-chain, and hen egg white lysozyme (HEWL) were purchased from Sigma Aldrich, U.K. and used without further purification.

(38) Timasheff, S. N. *Proc. Natl. Acad. Sci. U.S.A.* **2002**, *99*, 9721–9726.
(39) Webb, J. N.; Webb, S. D.; Cleland, J. L.; Carpenter, J. F.; Randolph, T. W. *Proc. Natl. Acad. Sci. U.S.A.* **2001**, *98*, 7259–7264.
(40) Wu, K.-P.; Kim, S.; Fela, D. A.; Baum, J. *J. Mol. Biol.* **2008**, *378*, 1104–1115.
(41) Uversky, V. N.; Cooper, E. M.; Bower, K. S.; Li, J.; Fink, A. L. *FEBS Lett.* **2002**, *515*, 99–103.
(42) Munishkina, L. A.; Cooper, E. M.; Uversky, V. N.; Fink, A. L. *J. Mol. Recognit.* **2004**, *17*, 456–464.
(43) Shtilerman, M. D.; Ding, T. T.; Lansbury, P. T. *Biochemistry* **2002**, *41*, 3855–3860.
(44) Munishkina, L. A.; Ahmad, A.; Fink, A. L.; Uversky, V. N. *Biochemistry* **2008**, *47*, 8993–9006.
(45) Arora, A.; Ha, C.; Park, C. B. *FEBS Lett.* **2004**, *564*, 121–125.
(46) Nielsen, L.; Khurana, R.; Coats, A.; Frokjaer, S.; Brange, J.; Vyas, S.; Uversky, V. N.; Fink, A. L. *Biochemistry* **2001**, *40*, 6036–6046.
(47) Dedmon, M. M.; Lindorff-Larsen, K.; Christodoulou, J.; Vendruscolo, M.; Dobson, C. M. *J. Am. Chem. Soc.* **2005**, *127*, 476–477.
(48) Guijarro, J. I.; Sunde, M.; Jones, J. A.; Campbell, I. D.; Dobson, C. M. *Proc. Natl. Acad. Sci. U.S.A.* **1998**, *95*, 4224–4228.

Quartz Crystal Microbalance Assay. All chemicals were purchased from Sigma Aldrich with the exception of methoxy terminated poly(ethylene glycol) thiol [$CH_3O(CH_2CH_2O)_6SH$] (Polypure, Norway). QSX 301 Standard Gold quartz sensors (mass sensitivity coefficient 17.7 ng cm^{-2} Hz^{-1}) were used throughout (Q-Sense, Sweden). All QCM measurements were made with a Q-Sense E4 instrument (Q-Sense, Sweden), and all AFM images with a PicoPlus AFM (Molecular Imaging, AZ).

The method of sensor preparation was varied depending on the pH required to attach the fibrils while maintaining their stability. Elementa common to all methods were probe sonication with 3 s pulses and 3 s rests to produce a uniform distribution of shortened seed fibrils of approximately 100 nm in length as determined by AFM, incubation of seed fibril suspensions on the sensor surfaces carried out in 100% humidity for 1 h, and passivation of all sensors by incubation with methoxy terminated PEG thiol (0.02%) in the appropriate buffer for 1 h.

All fibrils were prepared using procedures reported previously.[48−51] Specifically, PI3-SH3 fibrils were formed by incubation of a 10 mg/mL solution of the protein in 10 mM HCl at 40 °C for 4 days. The fibrils were diluted 5 times and activated by addition of cystamine and *N*-(3-dimethylaminopropyl)-*N*′-ethylcarbodiimide hydrochloride (EDC)[22] to final concentrations of 100 and 5 mM respectively. The fibrils were concentrated and resuspended twice by centrifugation at 12,000*g* for 2 h. The resulting pellet was diluted, sonicated, and incubated on the sensor as described above. α-Synuclein fibrils were formed by incubation of a 100 μM solution of α-synuclein in PBS buffer at pH 7.4 and 37 °C with stirring for 4 days, during which time the solution became cloudy. This solution was then concentrated by centrifugation at 10,000*g* for 15 min and then diluted 20 times and sonicated as above. The seeds were functionalized with 2-iminothiolane, added to a final concentration of 7.3 mM in order to attach them covalently to the gold surface. Insulin fibrils were formed by incubation of a 10 mg/mL solution of insulin from bovine pancreas in 10 mM HCl at 60 °C for 4 days, diluted 500 times, and sonicated as above. Insulin seed fibrils readily bind irreversibly to the gold surface of the sensor without the need for chemical modification. Hen lysozyme fibrils were formed by incubation of a 30 mg/mL solution in 10 mM HCl (pH 2.0) at 60 °C for 10 days. The fibrils were activated and incubated on the sensor as described above for PI3-SH3. Insulin B-chain fibrils were formed by incubation of a 10 mg/mL solution in 10 mM HCl (pH 2.0) at room temperature for 7 days. The resulting fibrils in each case were activated and incubated on the sensor as described for PI3-SH3.

Rheology. Measurements of high shear plateau solution viscosities for all cosolute solutions were made on an AR2000 stress controlled rheometer (TA Instruments, U.K.) at 25 °C with a 40 mm aluminum parallel plate geometry and 100 μm gap, recording at 5 points per decade.

Scaled Particle Theory. Scaled particle theory is used to provide a description of the volume fraction available to a particle upon its introduction into a bath of inert cosolute particles. From this volume fraction, the activity coefficients of reactants and products can be determined and the enhancement factor, Γ, can be calculated and used to obtain an elongation rate in crowded conditions relative to the elongation rate in an ideal solution. Minton has provided a rigorous thermodynamic background to the problem,[28] and this approach has also been used by Hatters et al.[29] According to scaled particle theory,[27] for the reaction

$$A + B \rightarrow (AB)^* \rightarrow AB \tag{1}$$

where A represents an amyloid fibril, B is the monomeric form of the protein, and AB is the elongated fibril following monomer addition, an enhancement factor, Γ, can be described using activity coefficients:

$$\Gamma = \frac{\gamma_A \gamma_B}{\gamma_{(AB)^*}} \tag{2}$$

where the activity coefficient of each species can be related to the volume available to it as

$$\gamma = \frac{1}{v_a} \tag{3}$$

The activity coefficients for a spherical monomer, A, a spherocylindrical seed fibril, B, and an elongated seed fibril, AB, can then be determined by calculating the volume available to each species in an inert polymer matrix according to scaled particle theory:[27]

$$\begin{aligned} \gamma_A &= \exp\left[\left(1 + \frac{r_p}{r_c}\right)^2 \upsilon c\right] \\ \gamma_B &= \exp\left[\left(1 + \frac{r_f}{r_c}\right)\left(1 + \frac{\Delta(i-1) + 2r_f}{2r_c}\right)\upsilon c\right] \\ \gamma_{AB} &= \exp\left[\left(1 + \frac{r_f}{r_c}\right)\left(1 + \frac{\Delta(i) + 2r_f}{2r_c}\right)\upsilon c\right] \end{aligned} \tag{4}$$

These equations may be combined according to eq 2 to give the length-independent enhancement factor, Γ:

$$\Gamma = \exp\left\{\left[\left(1 + \frac{r_p}{r_c}\right)^2 - \left(1 + \frac{r_f}{r_c}\right)\frac{\Delta}{2r_c}\right]\upsilon c\right\} \tag{5}$$

where r_p is the radius of the soluble protein prior to its conversion into an amyloid state, r_f is the radius of the amyloid seed fibril treated as a spherocylinder, r_c is the chain radius of dextran, υ is the specific exclusion volume of dextran (L/g), c is the concentration of dextran (g/L), and Δ is a proportionality constant related to the increase in fibril length upon addition of one monomer of protein to the spherocylinderical fibril. A similar equation can be derived for the same reaction in the presence of spherical cosolutes:

$$\Gamma = \exp\left\{\left[\left(1 + \frac{r_p}{r_c}\right)^3 - \left(1 + \frac{r_f}{r_c}\right)^2\frac{3\Delta}{4r_c}\right]\upsilon c\right\} \tag{6}$$

The rate constant for the reaction under crowded conditions can then be described as

$$k = k_0\Gamma \tag{7}$$

where k_0 is the rate constant in an ideal solution.

Acknowledgment. This work was supported by a BBSRC/Unilever CASE studentship (D.A.W.), in part by Programme Grants from the Leverhulme and Wellcome Trusts (C.M.D.), and by the EPSRC and IRC in Nanotechnology (M.E.W. and A.K.B.). T.P.J.K. is a Research Fellow at St John's College, Cambridge. We thank Carlos Bertoncini and Nunilo Cremades of the University of Cambridge for help with expression of α-synuclein and William J. Frith of Unilever Discover, U.K. for aid with rheological measurements and valuable discussions.

JA909997E

(49) Krebs, M. R.; Wilkins, D. K.; Chung, E. W.; Pitkeathly, M. C.; Chamberlain, A. K.; Zurdo, J.; Robinson, C. V.; Dobson, C. M. *J. Mol. Biol.* **2000**, *300*, 541–549.
(50) Bouchard, M.; Zurdo, J.; Nettleton, E. J.; Dobson, C. M.; Robinson, C. V. *Protein Sci.* **2000**, *9*, 1960–1967.
(51) Devlin, G. L.; Knowles, T. P. J.; Squires, A.; McCammon, M. G.; Gras, S. L.; Nilsson, M. R.; Robinson, C. V.; Dobson, C. M.; MacPhee, C. E. *J. Mol. Biol.* **2006**, *360*, 497–509.